

Impedance spectroscopy analysis on electrical properties of serpentine at high pressure and high temperature

ZHU Maoxu (朱茂旭)¹, XIE Hongsen (谢鸿森)¹, GUO Jie (郭捷)¹,
BAI Wuming (白武明)² & XU Zuming(许祖鸣)¹

1. Institute of Geochemistry, Chinese Academy of Sciences, Guiyang 550002, China;

2. Institute of Geology and Geophysics, Chinese Academy of Sciences, Beijing 100101, China

Correspondence should be addressed to Zhu Maoxu (email: Zhumaoxu@hotmail.com)

Received January 28, 2000

Abstract The electrical conductivity of serpentine is measured and the microscopic conductance mechanisms are investigated with impedance spectroscopy at 2.5–4.0 GPa and 220–780°C. The results show that the electrical conductivity is strongly dependent on the frequencies used, and that only arc I, which reflects grain interior conductance, occurs and dominates the whole conductance processes over 12–10⁵ Hz at high pressure before dehydration. The arc II, which indicates the grain boundary process, begins to occur at the initial stage of dehydration. After dehydration, due to the presence of highly conductive networks of free water, the electrical conductivity is not dependent on frequencies any longer and the total electrical conductivity is dominated by process of ionic conductance of free water in interconnected networks. Dehydration of serpentine enhances pronouncedly the total electrical conductivity, through which highly conductive layers (HCL) may be formed in the earth's interior.

Keywords: electrical conductivity, grain interior conductance, free water, dehydration, simulated experiments.

Experimental laboratory studies on electrical properties of materials of the deep earth at high temperature and high pressure not only provide proof for explaining the magnetotelluric field data and endue electrical conductivity-depths profiles constructed in terms of geophysical observations with mineralogical and petrological contents, but also bridge geophysics and geochemistry. There exist a series of highly conductive layers (HCL) in the earth's interior. Serpentine, which is one of the important hydrous minerals in subduction slabs, was regarded as one of the highly conductive minerals^[1]. Experimentally, the electrical properties of materials in the earth's interior are strongly dependent on point defect chemistry of minerals^[2], temperature and frequency used. Among them, the dependency on frequency is called frequency dispersion, which is caused by dielectric loss and polarization in the system of interest. In recent years, Roberts et al.^[3,4] experimentally studied the electrical properties of anhydrous minerals and partially-molten systems at high temperature and atmospheric pressure, and modeled the electrical conductance mechanisms with impedance spectroscopy. Huebner et al.^[5] experimentally investigated the potential effects on various conductance processes in anhydrous minerals at high temperature and high pressure. So far, however, the studies on the electrical properties of hydrous minerals, particularly during dehydration of hydrous minerals, have not been detailed. A lot of pervious experimental data for hydrous and anhydrous

minerals were obtained by direct current method or fixed single frequency alternative current one^[6–8], and the frequency dispersion effects were not taken into account. In this paper, the electrical conductivity for serpentine is measured at 2.5–4.0 GPa and 220–780°C, and the microscopic conductance mechanisms are investigated with impedance spectroscopy.

1 Samples and experimental method

All the samples were collected in Ailaoshan orogenic belt, Yunnan Province. The X-ray powder diffraction analysis shows that the samples are lizardite. All the experimental samples were ground into discs with 8 mm in diameter, 2.7 mm in thickness, and cleaned in acetone followed by cleansing ultrasonically in distilled water, then baked at 80–100°C for at least 6 h to eliminate adsorbed water before experiments.

All the experiments were carried out in YJ-3000 ton type apparatus. The details about the apparatus were described elsewhere^[9]. The sample assemblage is showed in fig. 1. Pyrophyllite cubes (32 mm×32 mm×32 mm) used as pressure medium and pyrophyllite tubes used as insulator medium were baked up to 500°C and 1000°C respectively to eliminate the potential effects of adsorbed and chemically bound water in the experimental system. Pyrophyllite tubes are 32 mm long, 13.5 mm in outer diameter and 8 mm in inner diameter. The electrodes are copper columns with 5 mm in diameter. The leads are copper wires. Pressure error is ± 0.01 GPa. Temperature is monitored by NiCr-NiAl thermocouple with an error of $\pm 5^\circ\text{C}$. The sensing junction of the thermocouple is placed near, but not in contact with, the samples. The section areas of the sample discs are bigger than those of the electrodes in order that surface electrical conductance can be minimized. The two-layered stainless steel foils used as heating elements are earthed to shield the surrounding electric noises. Pressure is increased to a desired value slowly and then remains constant, then temperature is increased step by step with an increment rate of 15°C/min in each step. At the end of each step the temperature remains constant long enough (30 min–1 h) to ensure an equilibrium state before measurement. The equilibrium state is assumed to obtain when the relative errors of the measured modulus, $|Z|$, is less than 5% at a given frequency within 5 min intervals. Then the modulus, $|Z|$, and phase angles, θ , are recorded simultaneously at 45 selected frequencies over the whole range of 12–10⁵ Hz with a ZL5 type LCR meter. The errors of $|Z|$ and θ are believed to be less than 0.5%.

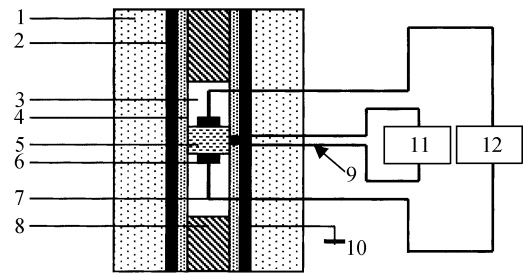


Fig. 1. The setup of sample assemblies. 1, Pressure medium; 2, heating elements; 3, boron nitride (BN) powder; 4, pyrophyllite insulator medium baked up to 1000°C; 5, sample; 6, electrode; 7, lead wire; 8, pyrophyllite spacer baked up to 1000°C; 9, thermocouple; 10, earthing; 11, differential thermometer; 12, LCR meter.

2 Results and discussion

2.1 Impedance spectroscopy principle

Impedance is the total opposition to current flow in response to an AC signal and is a complex quantity. Impedance consists of a resistance and a capacitance (R, C). The complex impedance, Z^* , is given by

$$Z^* = Z' - jZ'' \quad (1)$$

where Z' is real part and Z'' imaginary part. $j = \sqrt{-1}$. Z' and Z'' are determined at a given frequency by

$$Z' = |Z| \cos \theta \quad (2)$$

$$Z'' = |Z| \sin \theta \quad (3)$$

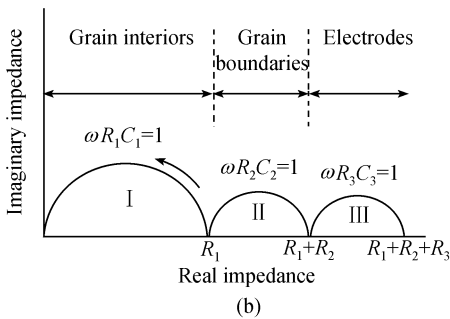
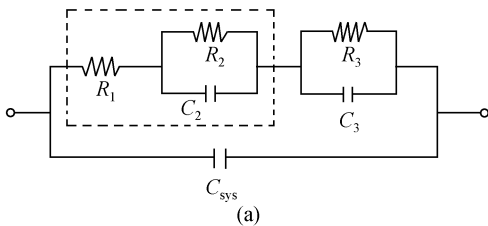


Fig. 2. The general form of the equivalent circuit used to model the overall response observed in single, polycrystalline, partially-molten, and dehydrated samples (a), and the equivalent circuit producing 3 impedance arcs in the complex plane (b). The system capacitance, C_{sys} , masks the smaller C_1 , according to Roberts et al.^[4] (see text for the details and discussion).

The experimental impedance data can be analyzed with impedance spectroscopy and equivalent circuits to extract the parameters (R, C) corresponding to specific conductance and polarization mechanisms. Fig. 2 shows the ideal forms of the equivalent circuit (a) and impedance spectra (b). R_1, R_2 and R_3 are resistors, C_{sys}, C_2 and C_3 are capacitors. Arc I, which stands for grain interior conductance mechanism, is equivalent to parallel $R_1 C_1$ (generally, the value of C_1 is much smaller than that of C_{sys} and therefore is masked by the latter one). Arc II, which stands for grain boundary mechanism, is equivalent to parallel $R_2 C_2$. Arc III, which stands for sample/electrode mechanism, is equivalent to parallel $R_3 C_3$. The center points of the three arcs are thought to be on the real axis. Generally, due to different relaxation times, τ ($\tau = RC$), the three

mechanisms above may occur over different frequency ranges, and, correspondingly, the arcs I, II and III may occur at high, middle and low frequencies, respectively. The complex impedance of single parallel RC is given by

$$Z^* = R / (1 + j\omega RC) \quad (4)$$

where $\omega = 2\pi f$ (f is frequency). In reality, in most cases, the center points of arcs fall below the real axis in the complex plane, rather than just on it due to distribution of relaxation times in the system of interest. In this case, the ideal equivalent circuit needs to be modified by introducing a

constant phase element (CPE) to substitute for C . The complex impedance of single parallel R -CPE is given by

$$Z^* = R/[1 + RC(j\omega)^\varphi]. \quad (5)$$

When $\varphi = 0$, the CPE behaves as an ideal resistor; when $\varphi = 1$, the CPE behaves as an ideal capacitor. Experimentally, φ is found to be between 0 and 1. The width of each arc on the real axis is equal to the value of the corresponding resistor of the parallel RC circuit element. This width on the real axis is extremely important because no assumptions are required to obtain the resistance value. R and C can be obtained by fitting the experimental data with a complex nonlinear least square (CNLS) method. Obviously, only Arcs I and II are related to the intrinsic electrical properties of the samples (shown in dash box in fig. 2). The electrical conductivity, σ , with respect to specific mechanism is calculated by

$$\sigma = (d/s)/R, \quad (6)$$

where d is the thickness of the samples, s , the section area of the electrodes. The previous studies show that 1–3 impedance arcs may occur for silicate minerals at high temperature and high pressure^[3]. Theoretically, three separate arcs may occur for polycrystalline as long as the frequencies used are wide enough and $\tau_1 \ll \tau_2 \ll \tau_3$ is satisfied. As for single crystal, there exist only two arcs due to absence of the grain boundary process. However, it should be noted, according to Huebner et al.^[5], that although the grain interior process is almost unaffected after suffering a high pressure, the grain boundary and sample/electrode process are greatly diminished.

2.2 Impedance spectroscopy

Fig. 3 shows the relationship of frequencies against phase angles at various temperatures. It is evident that the phase angles are strongly dependent on the frequencies used at relatively low temperatures, whereas the dependency becomes weak at elevated temperatures. The phase angles approximate zero when the temperatures are above 500–600°C at all pressures, which indicates that the phase angles are almost independent of the frequencies. When the temperature is up to 610°C, the phase angles are only weakly dependent on the frequencies used, particularly below 40 kHz, which implies that the electrical conductivity is also weakly dependent on the frequencies used. The dehydration temperatures of serpentine are believed to be 500–600°C in terms of varying chemical compositions^[10]. This temperature range

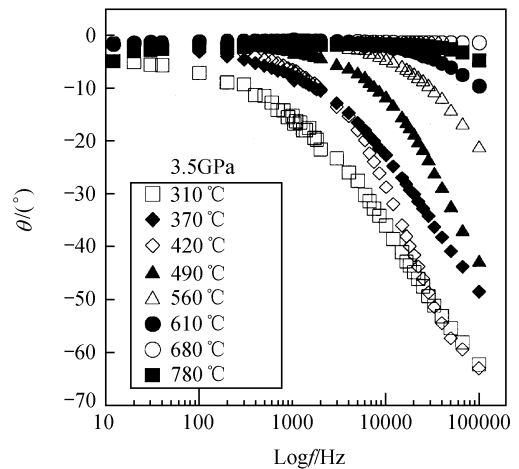


Fig. 3. The relationship between phase angles and frequencies at 3.5 GPa and various temperatures.

is roughly in accordance with the temperature at which the dependence of the phase angles on the frequencies disappears. It implies that dehydration makes the dependence of the phase angles on the frequencies weak or absent. Consequently the dependence of the electrical conductivity on the frequencies also disappears over this temperature range. It is most likely that this phenomenon is caused by forming highly conductive networks of free water in the system after dehydration. The similar behavior was reported by Duba et al.^[11] who investigated the electrical conductivity of rocks in which there exist some highly conductive solid phases, for example, graphite.

According to discussion above, only the impedance data before dehydration are analyzed with CNLS in $Z'-Z''$ complex planes to obtain R and C by fitting. The electrical conductivity after dehydration, due to the weak dependence of electrical conductivity on frequencies, is calculated with measured $|Z|$ and θ at 1 kHz by^[12]

$$\sigma = (d/s)(\cos\theta / |Z|), \quad (7)$$

Fig. 4 (a)—(e) shows the impedance spectra in $Z'-Z''$ complex planes at 3.5 GPa and 310—560°C. It can be seen that the values of both the real and imaginary parts decrease with increasing temperatures. At relatively low temperature there exists a semicircle which crosses through the origin and is centered below the real axis (see the values for φ). This semicircle, according to the principle of impedance spectroscopy^[13], indicates that the grain interior mechanism is predominant over the frequency range of 12—10⁵ Hz. Arcs II and III are out of our frequency range, which otherwise would have occurred if the frequencies used in our experiment were low enough. For example, Roberts et al.^[3] identified Arc II over frequency range of 10⁻³—10⁻⁴ Hz at high temperature and atmospheric pressure. Arc I becomes incomplete in a higher frequency region, however the Arc II begins to occur, which is not obvious at the similar frequency range as the temperature is increasing (fig. 4(b) and (c)). It suggests that Arcs I and II will shift to occur toward higher frequencies as the temperature is increasing. Similar results were reported by Duba et al.^[14]. Thus the dependency of electrical conductivity on frequencies needs to check to ensure a similar electrical behavior at various temperatures when determining the relationship of $\text{Log}\sigma$ against $1/T$ at a fixed frequency, otherwise data comparisons between laboratories will probably be meaningless. At 490°C and 560°C, Arc II, which reflects grain boundary process, is more obvious than that at lower temperatures. Thus we believe that there exist two main conductance processes over frequency range of 12—10⁵ Hz. Before dehydration, the grain boundary processes, as suggested previously^[15], are dominated by the impurity point defects at grain boundaries. After dehydration, initially released free water distributes as isolated pockets at grain boundaries, subsequently forms highly conductive networks. In this case, the boundary process is dominated by ionic conductance in free water. It can be inferred that Arc II mainly reflects conductance mechanism of free water around grain boundaries^[16]. We gave the typical impedance spectrum results at 3.5 GPa and various temperatures in fig. 4. The results at 2.5 GPa and 4.0 GPa are similar (not shown). The

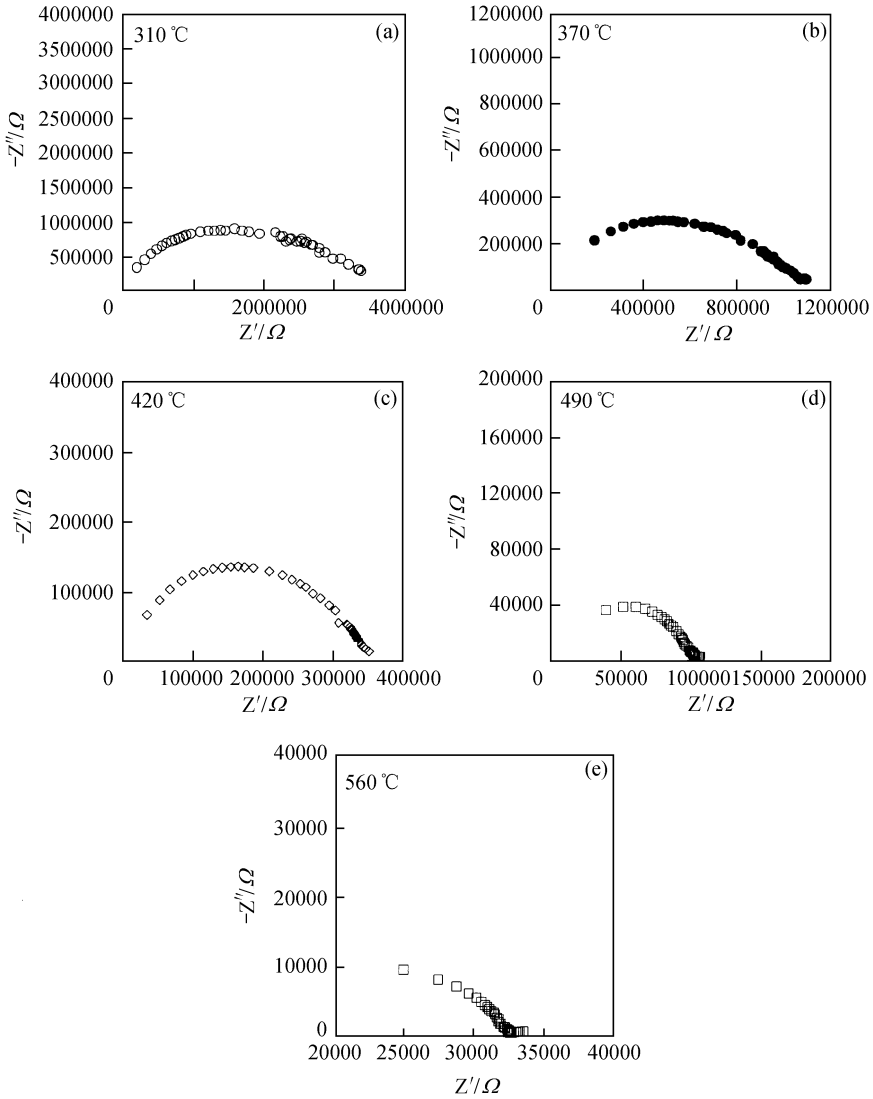


Fig. 4. $Z'-Z''$ impedance spectrum planes for serpentine at 3.5 GPa and various temperatures.

grain boundary conductivity, σ_{gb} , in both cases of fluid-free and isolated fluid-present, according to Roberts et al.^[3], acts in series with grain interior conductivity, σ_{gi} , i.e.

$$1/\sigma_T = 1/\sigma_{gb} + 1/\sigma_{gi}, \tag{8}$$

where σ_T is the total electrical conductivity. σ_T is smaller than both σ_{gb} and σ_{gi} , which implies that the total electrical conductivity is decreased in case of existence of grain boundary conductance. Once the free water forms interconnected networks, σ_{gb} acts in parallel with σ_{gi} ^[4], i.e.

$$\sigma_T = \sigma_{gb} + \sigma_{gi}. \tag{9}$$

Due to high conductance feature of free water, $\sigma_{gb} \gg \sigma_{gi}$ holds after dehydration. Consequently

σ_T is controlled by σ_{gb} , indicating that the bulk electrical conductivity of serpentine after dehydration is dominated by the charge carriers in the free water networks. The values of R_1 and C_1 are determined by fitting with CNLS. The fit parameters at 2.5 GPa, 3.5 GPa and 4.0 GPa are shown in table 1. The electrical conductivity of grain interior processes can be calculated by using R_1 and

Table 1 The fit parameters for serpentine at 2.5, 3.5 and 4.0 GPa and various temperatures with impedance spectroscopy

2.5 GPa				
T/K	R_1/Ω	C_1/F	φ	τ_1/s
493	1.411×10^7	2.719×10^{-10}	0.6773	3.837×10^{-3}
553	2.089×10^6	7.139×10^{-10}	0.6303	1.491×10^{-3}
623	3.650×10^5	2.009×10^{-9}	0.5915	7.333×10^{-4}
683	6.784×10^4	4.537×10^{-9}	0.5602	3.078×10^{-4}
3.5 GPa				
583	3.249×10^6	3.013×10^{-10}	0.6667	9.789×10^{-4}
643	1.062×10^6	4.845×10^{-10}	0.6511	5.145×10^{-4}
693	3.446×10^5	1.825×10^{-10}	0.8355	6.289×10^{-5}
763	1.031×10^5	3.317×10^{-10}	0.7960	3.420×10^{-5}
833	3.289×10^4	2.934×10^{-10}	0.8121	9.650×10^{-6}
4.0 GPa				
563	8.460×10^6	1.403×10^{-10}	0.7476	1.187×10^{-3}
658	6.518×10^5	2.523×10^{-10}	0.7380	1.645×10^{-4}
713	1.992×10^5	4.460×10^{-10}	0.7140	8.884×10^{-5}
773	6.491×10^4	3.257×10^{-10}	0.7561	2.114×10^{-5}
823	1.994×10^4	4.520×10^{-8}	0.3966	9.013×10^{-4}

eq. (6). The values of R_2 and C_2 cannot be resolved reliably with CNLS because of too few data for arc II in most cases, however. Thus we cannot exactly obtain σ_T . Nevertheless, Huebner et al.^[5] experimentally found that the grain interior processes are generally insensitive to confined pressure, however increasing pressure can substantially depresses both the grain boundary and sample/electrode processes. Consequently, grain interior process dominates the bulk conductivity. In comparison, this feature is also believed to hold for the earth's minerals at the depth of the mid or lower crust. Thus σ_{gi} can roughly be regarded as σ_T without much deviation before dehydration in our experiments. Roberts et al.^[3] contended that the investigation of electrical properties for polycrystalline silicate minerals over frequency range of 10^2 — 10^{-5} Hz is of importance because the grain boundary processes are believed to be significant over this range, and the frequencies used in magnetotelluric field measurements are also within the range. However, it should be noted that the conclusion of Roberts et al.^[3] was drawn based on experimental results at high temperatures and atmospheric pressures. Virtually, the grain processes are significantly diminished under confined pressure over this frequency range, and the grain interior processes are still dominant ones. In contrast, the dependence of electrical conductivity on frequencies together with $\sigma_{gb} \gg \sigma_{gi}$ makes $\sigma_T \approx \sigma_{gb}$ hold after dehydration. The relationship between $\text{Log}\sigma_T$ and $1/T$ is shown in fig. 5. It can be seen from fig. 5 that $\text{Log}\sigma_T$ against $1/T$ is well linear, i.e., $\text{Log}\sigma_T$ against $1/T$ can be well fitted by Arrhenius equation (eq. (10))

$$\sigma = \sigma_0 \exp(-\Delta E / kT), \quad (10)$$

where σ_0 is preexponential factor, T absolute temperature, k Boltzman constant and ΔE activation energy. The electrical conductivities of serpentine at 3.5 GPa and 4.0 GPa before dehydration are almost equal to each other at the same temperatures. They are 0.6 Log units higher than at 2.5 GPa, however the differences between them disappear after dehydration. Even though there were experimental observations to suggest that the differences of 0.5 Log units in the same experiments can be distinguished and attributed to some intrinsic affecting factors^[17] and most authors suggested that the differences to such extent are still within the laboratory errors^[8,18]. Thus it is difficult to distinguish whether such differences in our experiments are caused by confined pressures or by experimental error. However, due to such small differences, it can be sure that the effect of pressures above 2.0 GPa on electrical conductivity, if any, is small, which is basically in agreement with the result that the effect of pressure on electrical conductivity of silicate minerals is negligibly small^[18]. The slopes, i.e. ΔE , in fig. 5 are broken above 480—560°C, implying that the conductance mechanism changes from one dominant one to another. The electrical conductivity increases more rapidly with increasing temperature over this range of temperatures than at lower temperatures. The range of temperatures at which the slopes are broken is roughly in agreement with the range of temperatures at which serpentine dehydrates. It is most likely that dehydration causes the increases in the electrical conductivity and changes of the conductance mechanism because it is well established that the presence of little free water in the system can significantly enhances the total electrical conductivity of minerals. The presence of free water in the system can also result in the dominant electronic conductance to ionic one. After dehydration, the electrical conductivity of serpentine reaches 0.01—0.1 S/m, the values for typical HCL, implying that dehydration of minerals at high temperature and/or high pressure in subduction zones may be one of important candidates of geneses for forming HCL^[20].

The electrical conductivity of serpentine is below 10^{-5} S/m at 300°C, and below 10^{-3} S/m at 500°C. It suggests that the electrical conductivity of serpentine is low at relatively low temperature. However this conclusion is not in agreement with that of Stesky et al.^[1] who obtained electrical conductivity of 0.01—0.1 S/m for serpentinized basalt at room temperature and up to 0.6 GPa, which is several orders of magnitude higher than for serpentinized-free basalt. Thus they concluded that serpentine is a highly conductive mineral. However their samples contain a lot of

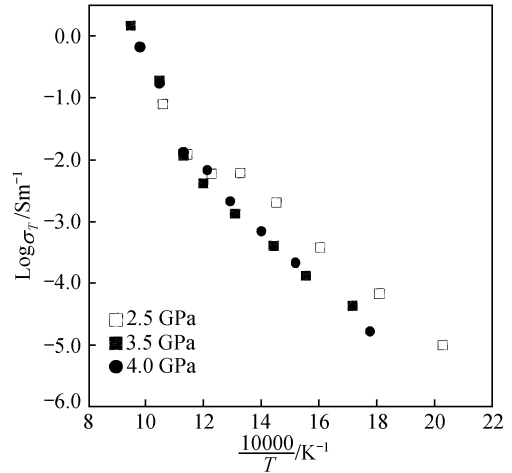


Fig. 5. The relationship between $\text{Log} \sigma_T$ and $1/T$ at 2.5 GPa, 3.5 GPa and 4.0 GPa for serpentine.

magnetite, a highly conductive solid phase, on the boundaries of minerals and the magnetite is well interconnected with each other on average. That would enhance significantly the bulk electrical conductivity of rocks due to its high electrical conductivity of 10^4 S/m^[21], which is several orders of magnitude higher than that of silicate minerals. Obviously, magnetite is not found on the boundaries of our samples under microscopic examinations. This may be the main cause for the discrepancies between our results and Stesky's et al.^[1] If the amount of magnetite in our samples was equivalent to that of Stesky et al., the electrical conductivity of our samples would be much higher than theirs because magnetite would reconnect with each other under confined pressure, and consequently the connectivity of magnetite and therefore the bulk electrical conductivity of rocks are enhanced^[22]. In addition, Popp et al.^[19] observed that the electrical conductivity of serpentine remained almost unchanged with a range of 10^{-6} — 10^{-7} S/m at room temperature and with increasing confined pressures up to 200 MPa, which also implies that highly conductive solid phases are absent in their samples. All the evidences can lend support to the point that the electrical conductivity of serpentine free of highly conductive solid phases is low at room and relatively low temperature. In summary, the high electrical conductivity for individual serpentine samples is caused by the existence of some highly conductive solid phases on grain boundaries, for example, magnetite and graphite, etc, but not by serpentine itself. It can be deduced that the presence of some highly conductive solid phases in rocks would play a very important role in forming HCL in the earth's interior if the amount reaches the extent to which they are well interconnected.

3 Conclusion

Through impedance spectroscopy analysis on the electrical properties of serpentine we can conclude that the phase angles and electrical conductivity are strongly dependent on frequencies used before dehydration of serpentine. The dependency of electrical conductivity on the frequencies used needs to check to ensure similar electrical behavior at various temperatures when determining the relationship between $\text{Log}\sigma$ against $1/T$ at a single fixed frequency. Only arc I, which reflects grain interior conductance, occurs and dominates the whole conductance processes over 12 — 10^5 Hz before dehydration. Arc II begins to occur at the initial stage of dehydration. After dehydration, due to the presence of the highly conductive networks of free water, the phase angles and electrical conductivity are not dependent on frequencies used any longer and the total electrical conductivity is dominated by process of ionic conductance in interconnected networks of free water. The rate-process-control charge carrier species transfer from electrons to ions and the total electrical conductivity is enhanced pronouncedly due to dehydration, through which HCL may be formed in the earth's interior. The electrical conductivity of serpentine is generally low at ambient to relatively low temperatures when highly conductive solid phases are absent. Highly conductive solid phases, for example magnetite and graphite, may play a very important role in forming HCL in the earth's interior.

Acknowledgements This work was jointly supported by the National Natural Science Foundation of China (Grant Nos. 49672099, 49904005) and Open Laboratory of High Temperature and High Pressure Geodynamics, Chinese Academy of Sciences. We are indebted to Dr. Zhou Wenge for completing an X-ray powder diffraction analysis of serpentine, Dr. Zhu Jianming for processing parts of the diagrams, Dr. Xu Yousheng in Bayreuth Geoinstitut, Universitat Bayreuth, Germany, for providing the CNLS software programmed by Bernard A. Boukamp.

References

1. Stesky, R. M., Brace, W. F., Electrical conductivity of serpentinized rocks to 6 kilobar, *J. Geophys. Res.*, 1973, 78 (32): 7614—7621.
2. Zhu Maoxu, Xie Hongsen, Experimental studies on electrical properties of materials in the earth's interior, *Advancement in Geosciences (in Chinese)*, 1998, 13(5): 438—446.
3. Roberts, J. J., Tyburczy, J. A., Frequency dependent electrical properties of polycrystalline olivine compacts, *J. Geophys. Res.*, 1991, 96 (B10): 16205—16222.
4. Roberts, J. J., Tyburczy, J. A., Frequency dependent electrical properties of minerals and partial-melts, *Surv. Geophys.*, 1994, 15: 239—262.
5. Huebner, I. S., Dillenburg, R. G., Impedance spectra of hot, dry silicate minerals and rock: Qualitative interpretation of spectra, *Amer. Mineral*, 1995, 80: 46—64.
6. Kavner, A., Li, X-Y, Jeanloz, R., Electrical conductivity of a natural (Mg, Fe)SiO₃ majorite garnet, *Geophys. Res. Lett.*, 1995, 22 (22): 3103—3106.
7. Hicks, T. L., Secco, R., Dehydration and decomposition of pyrophyllite at high pressure: Electrical conductivity and X-ray diffraction studies to 5 Gpa, *Can. J. Earth Sci.*, 1997, 34: 875—882.
8. Li, X-Y, Jeanloz, R., Effect of iron content on the electrical conductivity of perovskite and magnesio-wustite assemblages at lower mantle condition, *J. Geophys. Res.*, 1991, 96(B4): 6113—6120.
9. Xie Hongsen, *Introduction to the Materials in the Earth's Interior (in Chinese)*, Beijing: Science Press, 1997, 42—53.
10. Taturmi, Y., Migration of fluid phase and genesis of basalt magmas in subduction zone, *J. Geophys. Res.*, 1989, 94: 4697—4707.
11. Duba, A., Huenges, G., Nover, E. et al., Impedance of black shale from munsterland 1 borehole: An anomalously good conductor? *Geophys. J.*, 1988, 94: 413—419.
12. Watanabe, T., Kurita, K., The relationship between electrical conductivity and melt fraction in a partially molten simple system: Archie's law behavior, *Phys. Earth Planet Inter.*, 1993, 78: 9—17.
13. Macdonald, J. R., Johnson, W. B., *Fundamentals of impedance spectroscopy*, in *Impedance Spectroscopy* (ed. Macdonald, J. R.), New York: John Wiley & Sons, 1987, 1—26.
14. Duba, A., Constable, S., The electrical conductivity of lherzolite, *J. Geophys. Res.*, 1993, 98(B7): 11885—11899.
15. Roberts, J. J., Tyburczy, J. A., Frequency dependent electrical properties of dunite as functions of temperature and oxygen fugacity, *Phys. Chem. Minerals*, 1993, 19: 545—561.
16. Sato, H., Ida, Y., Low frequency electrical impedance of partially molten gabbro: The effect of melt geometry on electrical properties, *Tectonophysics*, 1984, 107: 105—134.
17. Xu, Y-S, McCammon, C., Poe, B. T., The effect of alumina on the electrical conductivity of silicate perovskite, *Science*, 1998, 282: 922—924.
18. Li, X-Y, Ming, L-C, Manghnani, M. H. et al., Pressure dependence of the electrical conductivity of (Mg_{0.9}Fe_{0.1})SiO₃ perovskite, *J. Geophys. Res.*, 1993, 98(B1): 501—508.
19. Popp, T., Kern, H., Thermal dehydration reactions characterised by combined measurements of electrical conductivity and elastic wave velocities, *Earth Planet Sci. Lett.*, 1993, 120: 43—57.
20. Gu Zhijuan, Guo Caihua, Li Biao et al., Primary studies on the genesis of the low-velocity and highly conductive layers in the crust, *Science in China, Series B (in Chinese)*, 1995, 25(1): 108—112.
21. Duba, A., Heikamp, S., Meurer, W. et al., Evidence from borehole samples for the role of accessory minerals in lower-crustal conductivity, *Nature*, 1994, 357: 59—61.
22. Shankland, T. J., Duba, A. G., Mathez, E. A. et al., Increase of electrical conductivity with pressure as an indicator of conduction through a solid phase in midcrustal rocks, *J. Geophys. Res.*, 1997, 102(B7): 14741—14750.